

Structure Decomposition for the Luminous Disk Galaxies in the NGC 524 Group

M.A. Ilyina¹ and O.K. Sil'chenko¹

*Sternberg Astronomical Institute of the Lomonosov Moscow State University,
Moscow, Russia¹*

Members of the NGC 524 group of galaxies are studied using data obtained on the 6m telescope of the Special Astrophysical Observatory of the Russian Academy of Sciences, with the SCORPIO reducer in an imaging mode. Surface photometry has been carried out and parameters of the large-scale galactic components – disks and bulges – have been determined for the six largest galaxies of the group. A lower than expected percentage of bars and high percentage of ring structures were found. Integrated $B - V$ colours for a hundred of dwarf galaxies in the vicinity (within 30 kpc) of the six largest galaxies of the group have been measured. A considerable number of blue irregular galaxies with ongoing star formation is found among dwarf satellites of the lenticular galaxies of the group. The luminosity function for dwarf galaxies of the group suggests that the total mass of the group is not very high, and that the X-ray emitting gas observed around NGC 524 relates to the central galaxy and not to the group as a whole.

1 INTRODUCTION

Groups of galaxies are very suitable places to study there the role of interactions concerning the evolution of galaxies due to external factors. The probability of the development of gravitational tides during close passages is the highest for the galaxies in groups, due to both the presence of close neighbours and the low relative velocities of intragroup movements. Groups, especially massive ones, often contain hot (X-ray), diffuse gas, which interacts with the cool gas of the galaxies themselves; such gas-dynamical interaction is usually considered as a reason for the dearth of cool gas in disk galaxies that are members of groups.

So-called “external secular evolution” (see the review by [1]) is a slow change of the global properties of galaxies caused by external factors. Secular evolution leaves certain imprints on the large-scale structures of galaxies: the radial density profiles of their disks become more complex, and additional structural components, such as bars, rings, and circumnuclear disks, arise in central regions. The dynamical properties of the stellar subsystems also change: the stellar disk becomes thicker (hotter) during the evolution, the vertical velocity dispersion of its stars increases, etc. Therefore, the origin of the large-scale structures of galaxies can be studied most effectively using a complex approach, beginning with the surface photometry, and then more clearly identifying the nature of the structural components with the spectral observations and kinematic measurements. In the present paper, which is the first in the series devoted to the nearby, rich NGC 524 group, we are starting with the surface photometry for a number of luminous member galaxies. The photometric data were obtained at the 6-m telescope of the Special

Astrophysical Observatory (SAO) of the Russian Academy of Sciences.

The NGC 524 group is well known, and has been studied for a long time, due to its location in a relatively sparsely populated area in the Northern sky. It was first cataloged by Geller and Huchra [2], when only eight galaxies were identified as members. Later, Vennik [3] found 18 luminous members and 13 dwarfs by undertaking an analysis of Palomar Atlas images using the force hierarchy clustering method, and Brough et al. [4] identified 16 members using the “friends-of-friends” algorithm. The NGC 524 group lists also 16 bright members in the last catalog of nearby galaxy groups by Makarov and Karachentsev [5]. Most of the bright members of the group are classified as lenticular galaxies; the fraction of early-type galaxies is estimated to be 0.56 ± 0.15 over the entire luminosity range [4]. The velocity dispersion of the group galaxies is about 180–190 km/s [3, 4], making the group fairly massive ($1.7 \cdot 10^{13} M_{\odot}$) and compact ($r_{500} = 0.26$ Mpc [4], $r_{500} = 0.42$ Mpc [6]). The ROSAT mission detected the X-ray emitting gas in the NGC 524 group, but since the radius of the detected X-ray spot is less than 60 kpc, the hot X-ray gas is thought to belong to the central galaxy of the group, NGC 524, and not globally to the group [7].

We have studied the structure of the six brightest galaxies of the group – four lenticulars and two early-type spirals – in detail. Their global characteristics retrieved from extragalactic databases are given in Table 1.

2 OBSERVATIONS

The photometric observations analyzed here were fulfilled at the prime focus of the 6-m telescope of the Special Astrophysical Observatory of the RAS with the SCORPIO reducer [11] operating in a direct-imaging mode. The

Table 1: Global characteristics of the galaxies under consideration

Galaxy	NGC 502	NGC 509	NGC 516	NGC 518	NGC 524	NGC 532
Morph.type (NED ¹)	SA0 ⁰ (r)	S0?	S0	Sa:	SA0+(rs)	Sab?
R_{25} , '' (RC3 ²)	34	43	39	52	85	75
B_T^0 (RC3)	13.57	14.20	13.97	13.56	11.17	12.91
M_B (RC3+NED)	-18.3	-17.7	-17.9	-18.3	-20.7	-19.0
$(B - V)$ (RC3)	0.91	-	-	-	1.00	0.80
V_r , km/s (NED)	2489	2274	2451	2725	2379	2361
Group center separation ^{3,2} , kpc	282	151	68	101	0	126
Distance to the group ⁴ , Mpc				24		

¹NASA/IPAC Extragalactic Database

²Third Reference Catalogue of Bright Galaxies [8]

³Sengupta & Balasubramanyam (2006), [9]

⁴Tonry et al. (2001), [10]

CCD-detector EEV 42-40 had a 2048×2048 format with a pixel size of $13.5 \mu\text{m}$; the readout was performed in a double-binned regime, yielding a sampling of $0.35'' - 0.36''$ per pixel. The total field of view of the reducer was $6.1' \times 6.1'$. The observations were carried out in the standard Johnson B and V bands. An exposure of twilight sky was used as a flat field. A detailed log of observations is presented in Table 2. Observations of the NGC 524 group were performed on the night of 21/22 August, 2007, under photometric conditions with a seeing of about $2''$. We took BV -band exposures of six fields centered onto the brightest galaxies of the group: NGC 524, NGC 502, NGC 509, NGC 516, NGC 518, and NGC 532. We used the exposures of the central galaxy of the group, NGC 524, as a photometric standard; the HYPERLEDA database contains a good set of aperture photoelectric data for this galaxy reduced to the standard Johnson system.

Table 2: Photometric observations of the NGC 524 group

Field center	Band	Total exposure, s	Seeing
NGC 502	<i>B</i>	540	2.3''
NGC 502	<i>V</i>	240	2.1''
NGC 509	<i>B</i>	540	2.0''
NGC 509	<i>V</i>	300	2.0''
NGC 516	<i>B</i>	540	2.2''
NGC 516	<i>V</i>	240	2.0''
NGC 518	<i>B</i>	540	1.9''
NGC 518	<i>V</i>	240	2.1''
NGC 524	<i>B</i>	60	1.8''
NGC 524	<i>V</i>	30	2.3''
NGC 532	<i>B</i>	360	1.8''
NGC 532	<i>V</i>	180	2.3''

3 STRUCTURE OF THE LARGE DISK GALAXIES IN THE NGC 524 GROUP

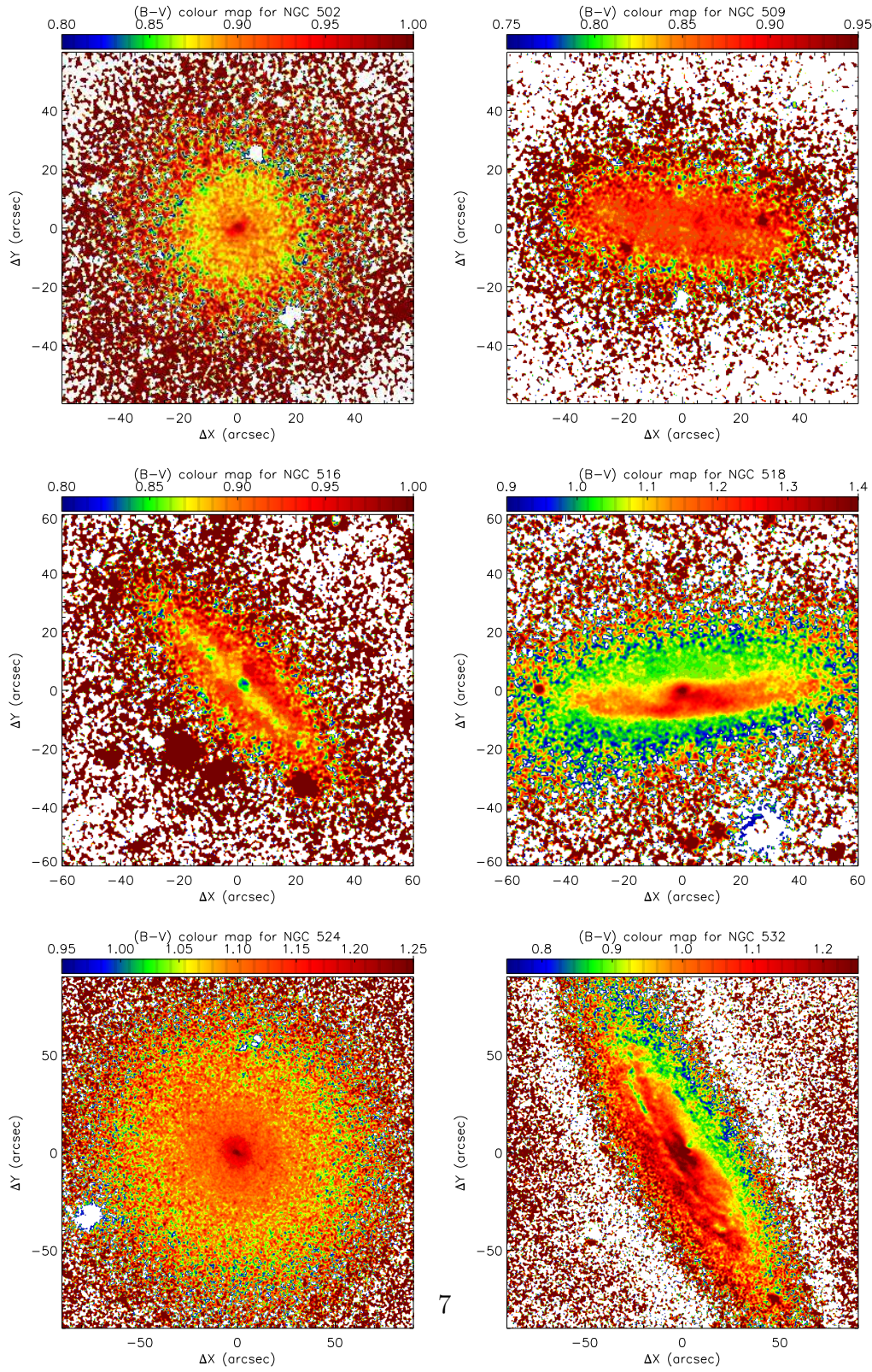
Figure 1 presents $B - V$ colour maps of the six brightest disk galaxies of the group. The lenticular galaxies NGC 524 and NGC 502 are viewed nearly face-on, and colour maps reveal very red nuclei, with the colours becoming bluer outward in a monotonic, axially symmetric fashion representing the classical radial colour gradient in early-type galaxies, usually interpreted as a gradient of the metallicity of the stellar population. On the contrary, the lenticular galaxies NGC 509 and NGC 516 are viewed edge-on. Unlike NGC 524 and NGC 502, their nuclei are bluer than the main bodies of the galaxies. Outside the nucleus, NGC 509 shows uniformly red colours without any noticeable trend with radius, while NGC 516 has a thin bluish disk embedded into a redder structure that can be taken as a thick stellar disk. The colour maps

for the spiral galaxies NGC 518 and NGC 532 display strong dust lanes projected onto the bulges, which relate to the spiral arms of these galaxies; the shift of the projections of the dust arms relative to the nuclei along the minor axes confirms our isophotal analysis conclusion, that these galaxies are not viewed strictly edge-on, but under the inclination of approximately 80° .

We performed an isophotal analysis and determined the major-axis position angles and ellipticities of the isophotes as a function of radius for all six galaxies in both filters. As a rule, the isophote ellipticity reaches a plateau at some distance from the center and does not change further with radius. We assume that this level, $e \equiv 1 - b/a$, is related to the inclination of the galactic disk to the line of sight i as following

$$\sqrt{\frac{2e - e^2}{1 - q_0^2}} = \sin i$$

where q_0 takes into account the “thickness” of the disk and is equal to the scale height and scale length ratio, z_0/h . The radius where the ellipticity reaches a plateau borders the region where the thin outer stellar disk dominates in the total surface brightness of the galaxy. In this region, we can determine the scaling parameters of the exponential shape of the disk surface brightness profile [12] without including other structural components of the galaxy. Decomposition, i.e. a separation of the contributions of the spheroidal and disk components, is needed in more central regions. The behaviours of the isophote ellipticities in the central regions of NGC 524, NGC 502, and NGC 532 are more complex than is expected for the superposition of a spheroidal bulge and a flat disk. In NGC 524, the isophote ellipticity increases towards the center (Fig. 2,b), NGC 532 has a local maximum of the ellipticity at $r = 4 - 5''$ (Fig. 2,c), and NGC 502 has two local ellipticity max-



7

Figure 1: $B-V$ colour maps for the six large galaxies of the NGC 524 group.

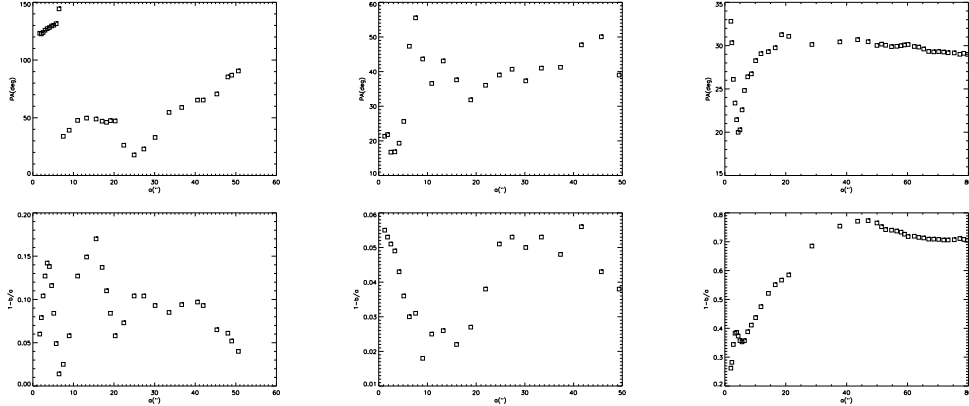


Figure 2: Results of our isophotal analysis of the V images for a – NGC 502, b – NGC 524, and c – NGC 532. The radial dependencies of the major-axis position angle (top) and the ellipticity of the isophotes (bottom) are shown.

ima at radii of $4''$ and $15''$ (Fig. 2,a). The position angle also has a distinct value near local maxima of the ellipticity: the major axis of the isophotes turns relative to the line of nodes of the galactic planes. This behaviour of the isophotes implies the presence of inner structures in the central regions of these galaxies, such as compact minibars, or even tilted circumnuclear disks. The large-scale structure of the galaxies was analyzed using the GIDRA software [13], fed with the orientation parameters of the isophotes obtained above. The surface brightness profiles were constructed by averaging counts in elliptical rings, with a fixed center at the galactic nucleus, and with the major axis and ellipticity corresponding to the isophotes at a given radius. The resulting profiles were then iteratively decomposed into an exponential disk (or disks) and a Sersic bulge, starting from the outermost regions. This approach is not suitable for galaxies viewed edge-on, such as NGC 509 and NGC 516; for them, we made two linear cuts, along the major and minor

Table 3: Parameters of photometric components

Galaxy	Band	Outer disk			Inner disk			n	Bulge		
		μ_0 , mag/ \square''	r_0''	r_0 , kpc	μ_0 , mag/ \square''	r_0''	r_0 , kpc		μ_0 , mag/ \square''	r_0''	r_0 , kpc
NGC 502	<i>B</i>	24.6	44.7	5.2	21.2	9.9	1.2	1.5	17.1	3.4	0.4
NGC 502	<i>V</i>	~23	39.3	4.6	20.1	10.5	1.2	1.5	15.8	3.53	0.4
NGC 509	<i>B</i>	20.6	33	3.8	–	–	–	1.5	17.4	3.0	0.35
NGC 509	<i>V</i>	19.6	33	3.8	–	–	–	1.5	16.2	2.8	0.3
NGC 516	<i>B</i>	23.0	24	2.8	19.8	11.5	1.3	1.8	17.9	3.0	0.35
NGC 516	<i>V</i>	21.9	29	3.4	18.5	13	1.5	1.9	16.6	2.84	0.3
NGC 518	<i>B</i>	22.9	34.4	4.0	21.2	16.4	2.0	2	17.1	8.2	0.95
NGC 518	<i>V</i>	21.6	35.4	4.1	19.8	16	1.9	2	16.4	6.67	0.8
NGC 524	<i>B</i>	21.5	30.9	3.6	19.5	9.0	1.05	1.2	17.9	3.1	0.4
NGC 524	<i>V</i>	20.3	30.9	3.6	18.3	8.6	1.0	1.2	16.6	2.8	0.3
NGC 532	<i>B</i>	20.8	70.2	8.2	19.45	18.7	2.2	2	17.0	6.0	0.7
NGC 532	<i>V</i>	20.45	73.2	8.5	18.2	20.5	2.4	2	15.7	4.8	0.55

axes, instead of averaging the surface brightness in rings. The cut along the minor axis was then used to estimate the bulge parameters, and the cut along the major axis was decomposed into the (already determined) bulge and second-order Bessel function(s) corresponding to the line-of-sight integral of the surface brightness of a round exponential disk that is optically thin up out to its edge. Table 3 presents the parameters of the large-scale structural components derived in such a way.

Below we give comments on the decomposition results for the individual galaxies.

NGC 502.

The center of this galaxy demonstrates a very interesting structure: at first glance it seems that two bars of different scales are embedded into each other (see also Fig. 2,a). We were able to trace the outer disk of the galaxy from the radius of $70''$: it is a low surface-brightness disk. A residual surface-brightness profile obtained after subtracting the first model disk from the original image has two “holes”, typical for a Freeman Type

II profile. We fitted this residual profile using a second model disk in the interval from $23''$ to $60''$, assuming that there is a brightness excess, a ring, between $R = 33''$ and $R = 45''$. After subtracting the second model disk, the residual profile has a noticeable “hump” between $10''$ and $24''$. Basing on the assumption that the galaxy contains two exponential disks and a Sersic bulge, we fitted this profile with a somewhat flattened ($b/a = 0.91$) Sersic bulge with $n = 1.5$. The residuals obtained by subtracting the three-component model from the initial image suggest that there is a nuclear bar with a radius of $6.5''$ and a ring located approximately between $5.9''$ and $20''$, with some shallow brightness peak in the middle of this interval. Another possibility is that the central structure with a radius of $20''$ may be a lens; but then there is no place for a bulge in this galaxy. Further analysis of kinematic data is needed to distinguish between these alternatives.

NGC 509.

It appears that this galaxy is viewed edge-on, so that the *GIDRA* software cannot be used in this case. Unfortunately, a linear photometric cut can provide less information than a brightness profile averaged in rings (ellipses), due to the higher noise level, hindering “extension” of the profile to large distances from the galactic center. It is probably for this reason that we have distinguished only one exponential disk in the outer regions of this galaxy. The central regions of the profile, out to $9''$ from the nucleus, were fitted by a Sersic bulge with $n = 1.5$. The brightness profile has a prominent “hump”, or possibly a flat brightness profile, at radii from $9''$ to $44''$, as is typical of the lenses of S0 galaxies. A turn of the isophote major axis by 8° is visible in the radial dependency of the position angle at $R = 7'' - 30''$,

and the isophote ellipticity shows a maximum (0.7) within this radius range; further, out to the edge of the outer disk, the isophote ellipticity drops to 0.4. This region ($R = 7'' - 30''$) has a uniformly red colour. We can treat this inner component as a lens. Or it may be that NGC 509 is not viewed quite edge-on, and then the turn of the isophotes indicates that the lens is non-axisymmetric. The galaxy apparently possessed structures such as a bar and ring, which have dissolved somewhat and spread over azimuth by the current moment.

NGC 516.

This galaxy is viewed edge-on. Its surface brightness profile demonstrates a bend in the central region, as is typical for a Freeman Type II profile; this may indicate the presence of a bar in the galaxy. The maximum isophote ellipticity (0.7) is observed $20''$ from the center, supporting the hypothesis that a bar is present. The isophote ellipticity drops to 0.55 towards the galaxy's edge. However, a thin, blue, edge-on disk "embedded" into a thicker reddish component is visible in the colour map (Fig. 1), within about $25''$ of the center. It is possible that the brightness excess in this radius interval is due to the embedded young disk, and not to a bar, which would not look uniformly blue along the whole of its length.

We have tried to model the disk component of the galaxy basing on the approach described in [14, 15]. Note that the NGC 516 profile should be classified as a Type II profile. As a result, we have extracted outer and inner disks, as well as a bulge that dominates the surface brightness within $5''$ of the center.

NGC 518.

According to the HYPERLEDA data, the galaxy’s inclination is 82° . This is confirmed by the projection of the dust lane against the central region, which is clearly visible in the images and colour map. Our isophotal analysis shows a constant isophote ellipticity (0.65) starting from $R = 35''$ and toward the very edge of the disk. To obtain the surface-brightness profile, we applied a photometric cut along the major axis of the isophotes. A “hump” is visible in the profile between the radii of $10''$ and $37''$ which is most likely the result of the intersection of our linear cut with the spiral arms. We were able to fit the profile using two exponential disks and a Sersic bulge with $n = 2$.

NGC 524.

The outer disk of the central group galaxy can be fitted with a model exponential disk starting from $70''$. The residual profile between $11''$ and $35''$ should be fitted with an inner exponential disk. Multiple narrow rings extending to $R \approx 61''$ are clearly visible in the residual image. We continued to fit the residual image in the radial range of $R = 0 - 11''$ with an almost round Sersic bulge having a quasi-exponential profile ($n = 1.2$). Subtracting the total three-component model yields residuals containing a set of weak rings between $34''$ and $61''$, a bright ring at $R = 13'' - 25''$, and, possibly, an inclined nuclear disk (Fig. 3).

Laurikainen et al. [16] recently performed a two-dimensional decomposition of a K_S -band image of NGC 524 which was less deep than the image analyzed by us here. They traced an outer exponential disk to a radius of $80''$ and noted the presence of two exponential segments with different

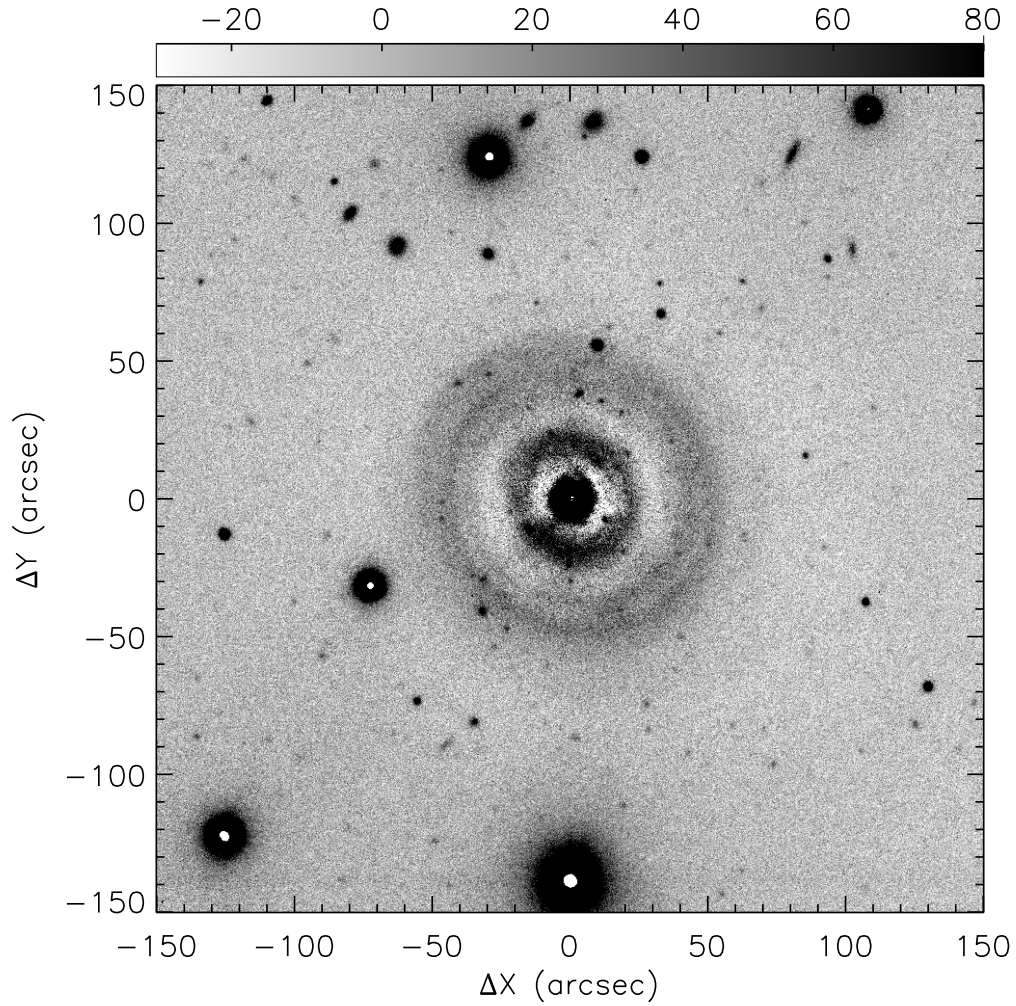


Figure 3: Residual V -band image for NGC 524 after subtraction of the 2D three-component model (two exponential disks and a Sersic bulge) from the initial image, showing rings at various radii in the surface-density distribution of the (old) stellar population.

scales in the residual profile within $R = 30''$. However, their model for the inner region consisted not of exponential disks, but of a Sersic bulge with $n = 2.7$ and two Ferrer's lenses with flat brightness profiles, every the latter compensating the steep slope of the bulge brightness profile within the radius ranges of $R = 0'' - 10''$ and $R = 10'' - 30''$. It is obvious that, mathematically, decomposition of the two-dimensional surface-brightness distribution into components admits more than one solution, especially if we do not restrict the number of components and their functional form. A final diagnostics – (pseudo-)bulge or thin disk dominates in the very center of NGC 524 – can be made only by using kinematical data: stellar disks are dynamically cooler than spheroids, and their stellar velocity dispersions should be lower than those in bulges and lenses. We have already carried out a kinematical analysis of the stellar component of NGC 524 at various distances from the center, and the kinematics indicates that the cool disk component dominates within $R = 10'' - 30''$ [17].

NGC 532.

The fit of the outer parts of this galaxy with an exponential disk can be started from $R = 125''$. The residual profile can be characterized as a Freeman's Type II profile. We have fitted this residual profile accurately using a model disk so as to retain the maximum information. After subtracting two exponential disks, spiral arms are clearly visible in the residuals. Further modelling adds a small, strongly flattened bulge ($b/a = 0.68$) with the Sersic parameter $n = 2$. It is difficult to extract details of the circumnuclear structure due to the high inclination and dust content of the galaxy.

4 DWARF GALAXIES OF THE GROUP

As a supplement to the surface photometry of the largest member galaxies of the group, we also performed two-colour aperture photometry of smaller galaxies within the $6'$ -fields around the main targets. We carried out photometry of all objects whose sizes exceeded the estimated full width at half maximum of the stellar images. After completing a list of extended objects, the BV colour map was made for every field (Fig. 1) and $B - V$ colours were measured for every list target within a $3'' - 4''$ aperture around each. Since most of these galaxies are dwarfs (or compact remote objects), their $3'' - 4''$ -aperture colours can be considered as the integral colours of the galaxies. The accuracy of the measured colours was estimated from the pixel-to-pixel scatters within the apertures used for the measurements (over 11×11 or 9×9 pixels), which ranges from 0.03^m for the brightest dwarfs to 0.2^m for the faintest. The BV colour index was corrected for the extinction in our Galaxy in accordance with [18] recommendations; $E(B - V) = 0.08$ was derived from the NED database. In general, 183 galaxies were measured in six fields.

Data of the SDSS-III survey covering a section of the sky containing the NGC 524 group became available over the Internet at the beginning of 2011, in particular, integrated *ugriz* photometry (so-called “Petrosian” magnitudes) became available at the site <http://skyserver.sdss3.org/dr-8/en/tools/explore/>. Although the SDSS-III photometry is less deep than our own photometry (as we have assured by comparing our $B - V$ colour maps and the SDSS-III *gr* colour maps for the large galaxies of the group), we have decided to use these data in order to

separate background galaxies from dwarf members of the group. The photometric redshifts for the galaxies having *ugriz* magnitudes are calculated in the SDSS databases. The calculation of photometric redshifts is based on a so-called “learning sample” – a list of galaxies for which both photometric and spectroscopic redshifts are available. Unfortunately, the learning sample contains no dwarf spheroidal or dwarf irregular galaxies, for which very few, if any, spectra have been obtained, even for the dwarfs in the nearby Universe, that severely hampers attempts to determine photometric redshifts for the dwarf members of the NGC 524 group.

Basing on the typical accuracy of photometric redshifts in the SDSS survey, 0.035, as given in [19], we rejected galaxies with the measured SDSS photometric redshifts having accuracies better than 0.07 (2σ) from our list of candidate dwarf galaxies of the NGC 524 group. We then verified “by eye” the morphology of the remaining candidates and required that the corrected $B - V$ colour should be bluer than 1.3. As a result, 97 objects have remained in the list of dwarf galaxies of the NGC 524 group, over the six fields analyzed, covering approximate radii of 30 kpc around the large galaxies of the group. For most of these, we converted the integrated SDSS g magnitudes to absolute B magnitudes using the relationship between the *ugriz* and *UBVRI* photometric systems given by [20]; for the galaxies without SDSS photometry, we measured the B magnitudes using our own data, taking fluxes in a series of rising apertures until the background level was reached beyond the outermost aperture. We then corrected the B magnitudes for the extinction in our Galaxy according to the recommendations of NED and converted these into the absolute magnitudes using the distance modulus to the group, 31.9 [10]. Final results for the entire list of

the measured dwarf galaxies are given in Table 4.

Table 4: Coordinates, absolute magnitudes, and the colours for the dwarf galaxies in the NGC 524 group

No. within the field	$\alpha_{2000.0}$	$\delta_{2000.0}$	M_B	$(B - V)_0$
The field of NGC 502				
1	01h 23m 04.3s	+09° 03' 35''	-10.92	1.26
2	01 22 58.4	+09 04 39	-9.88	0.96
3	01 22 48.8	+09 04 02	-10.08	0.98
4	01 22 48.0	+09 03 49	-10.50	0.69
5	01 22 47.6	+09 02 09	-9.98	0.85
6	01 22 52.6	+09 00 25	-8.97	1.17
7	01 22 58.2	+09 01 39	-9.85	0.68
8	01 23 05.3	+09 00 49	-8.59	0.82
9	01 23 05.0	+09 00 58	-9.27	1.09
10	01 23 04.6	+09 00 47	-9.66	0.78
11	01 23 00.0	+09 00 37	-9.40	1.11
12	01 22 53.0	+09 03 25	-10.17	0.83
The field of NGC 509				
1	01 23 28.4	+09 28 01	-10.55	0.63
2	01 23 27.3	+09 28 09	-8.93	0.32
3	01 23 27.9	+09 27 21	-9.55	0.98
4	01 23 23.4	+09 27 40	-11.52	0.93
5	01 23 13.1	+09 28 01	-9.87	0.32
6	01 23 16.9	+09 27 26	-8.81	0.36
7	01 23 20.3	+09 28 34	-9.53	0.60
8	01 23 19.8	+09 28 29	-8.69	0.55
9	01 23 20.8	+09 27 09	-9.03	0.34
10	01 23 23.7	+09 26 59	-9.05	0.48
11	01 23 19.8	+09 25 52	-10.35	0.95
12	01 23 14.2	+09 24 18	-9.90	0.44
13	01 23 24.1	+09 25 36	-10.21	0.63
14	01 23 24.4	+09 24 55	-10.28	0.70
15	01 23 28.0	+09 24 19	-9.25	0.58
16	01 23 32.3	+09 27 18	-10.32	0.66
17	01 23 28.6	+09 27 42	-9.65	0.52
18	01 23 27.0	+09 27 33	-9.60	1.00
19	01 23 21.6	+09 26 42	-10.77	0.61
20	01 23 19.7	+09 27 45	-9.58	0.38
21	01 23 24.6	+09 27 01	-8.82	0.93
22	01 23 24.6	+09 26 50	-11.22	0.46
The field of NGC 516				
1	01 24 11.0	+09 35 20	-11.29	0.86
2	01 24 15.6	+09 34 57	-9.37	1.09
3	01 23 59.6	+09 35 20	-9.88	0.72
4	01 24 05.6	+09 31 52	-9.71	1.00
5	01 24 14.6	+09 30 23	-9.06	1.18
6	01 24 12.7	+09 30 24	-9.20	0.58
7	01 24 06.1	+09 30 27	-10.67	0.94
8	01 24 18.2	+09 32 25	-9.97	0.73
9	01 24 16.0	+09 32 19	-9.00	1.25
10	01 24 06.8	+09 32 34	-11.43	1.13
11	01 24 06.7	+09 32 32	-10.97	1.10
12	01 24 15.6	+09 32 51	-9.62	0.84
13	01 24 16.2	+09 33 01	-9.41	0.94

No. within the field	$\alpha_{2000.0}$			$\delta_{2000.0}$			M_B	$(B-V)_0$
14	01	24	16.6	+09	33	08	-9.39	0.76
The field of NGC 518								
1	01	24	24.2	+09	20	58	-9.63	0.84
2	01	24	07.6	+09	21	06	-9.33	0.34
3	01	24	22.4	+09	18	27	-11.53	0.79
4	01	24	22.6	+09	17	17	-9.27	0.53
5	01	24	27.7	+09	18	27	-9.71	0.43
6	01	24	24.8	+09	17	08	-8.76	0.89
7	01	24	23.8	+09	17	30	-9.54	0.55
8	01	24	10.7	+09	22	01	-9.81	0.74
9	01	24	10.2	+09	21	52	-8.68	0.13
10	01	24	08.6	+09	20	02	-12.77	0.92
11	01	24	17.5	+09	21	21	-11.26	0.85
12	01	24	20.9	+09	22	22	-10.23	1.00
13	01	24	26.1	+09	17	53	-9.07	0.89
The field of NGC 524								
1	01	24	52.4	+09	34	22	-10.46	1.14
2	01	24	49.7	+09	33	49	-11.31	1.29
3	01	24	54.3	+09	34	09	-10.23	0.06
4	01	24	53.0	+09	34	03	-12.02	0.98
5	01	24	51.9	+09	33	52	-12.71	1.05
6	01	24	42.4	+09	34	25	-11.57	1.16
7	01	24	41.0	+09	33	50	-11.22	0.50
8	01	24	45.6	+09	33	38	-10.48	0.77
9	01	24	53.6	+09	31	23	-10.38	0.78
10	01	24	50.7	+09	30	51	-10.51	0.84
11	01	24	44.7	+09	29	35	-10.50	0.82
12	01	24	44.1	+09	29	56	-9.94	0.10
The field of NGC 532								
1	01	25	23.0	+09	16	51	-9.88	1.12
2	01	25	16.8	+09	18	28	-9.30	0.80
3	01	25	14.7	+09	18	34	-9.31	0.66
4	01	25	15.4	+09	18	01	-8.91	0.75
5	01	25	11.8	+09	16	52	-9.35	0.69
6	01	25	08.5	+09	15	19	-9.39	0.25
7	01	25	07.2	+09	15	17	-9.79	1.22
8	01	25	07.6	+09	15	02	-9.54	0.47
9	01	25	21.5	+09	13	24	-9.70	0.98
10	01	25	26.7	+09	13	22	-9.86	0.53
11	01	25	28.5	+09	13	29	-9.83	0.81
12	01	25	22.3	+09	13	03	-9.27	0.09
13	01	25	20.2	+09	14	37	-9.89	0.49
14	01	25	24.7	+09	15	01	-9.83	0.86
15	01	25	17.8	+09	14	28	-10.25	0.65
16	01	25	20.5	+09	13	44	-9.59	0.49
17	01	25	22.5	+09	13	43	-9.72	0.72
18	01	25	14.6	+09	18	16	-9.12	1.10
19	01	25	09.5	+09	18	08	-9.16	0.08
20	01	25	08.9	+09	14	04	-9.00	0.59
21	01	25	24.3	+09	13	34	-9.79	0.28
22	01	25	23.2	+09	13	25	-9.15	0.65
23	01	25	24.2	+09	14	10	-9.16	0.47
24	01	25	24.1	+09	14	26	-9.29	0.14

It is astonishing that our lists contain no galaxies brighter than $M_B =$

-13^m , and such galaxies were also not found in wider neighbourhoods of the studied fields, which we surveyed using a navigator of the eighth SDSS data release. Since the NED database does not detect also any such galaxies during a search for members of the group over the total area of the group, we conclude that there exists no group galaxies with the absolute magnitudes between $M_B = -13^m$ and -16^m , i.e., the luminosity function of the group galaxies is clearly bimodal. Figure 4 presents the luminosity function of the identified dwarfs and of the 16 large members of the group, for which we take the integrated blue magnitudes from [3]. Formally, we must match the two parts of the luminosity function – this for large and that for small galaxies, with a boundary near $M_B = -16^m$ – by multiplying the dwarf branch by a factor related to the fact that we have not studied the full area of the group. Assuming a uniform distribution of dwarf galaxies over the group area, this factor should be 35. However, Fig. 4 shows that so substantial correction is not needed, and the required factor does not exceed 10: apparently, the dwarfs are concentrated near the large galaxies, being satellites of the latter. Figure 4 also compares the luminosity function of the members of the NGC 524 group with the average luminosity functions of various-mass groups calculated in [21]. The slope of the dwarf branch is consistent with all the average luminosity functions (although it is shifted by several magnitudes toward the area of faint galaxies). In the bright part of the luminosity function, the number of galaxies in the NGC 524 group matches the luminosity functions of groups with zero or low X-ray luminosities (with low or intermediate total masses); however a bimodal luminosity function is exclusively a feature of groups without X-ray emitting gas at all [21]. The ROSAT data indicate an X-ray luminosity of $\log(L_X[\text{erg/s}]) = 41.05$ for the

NGC 524 group [7], but there is a note that the X-ray emission is tightly concentrated around the central galaxy, NGC 524. Now we see that the shape of the galactic luminosity function in the NGC 524 group supports the idea that the group itself *has no* hot intergalactic gas.

Figure 5 presents the $B - V$ colour distribution for the dwarf galaxies. This distribution is nearly flat in the colour interval of $B - V = 0.4 - 1.0$: we do not see the usual bimodality, with a “red sequence” and “blue cloud”. Although we could suppose, based on the example of our Local Group, that red dwarfs must be concentrated near large host galaxies and blue dwarfs are mostly located far from such galaxies: as a rule, tidal effects from large galaxies must suppress star formation in their satellites over dynamical timescales. However, in the case of the NGC 524 group, a considerable number of blue dwarfs with star formation were found just near the large galaxies.

The colour–luminosity diagram in Fig 6 compares the dwarf populations of the NGC 524 group and that of the Local Group (the data for the Local Group were taken from [22]). Dwarfs of both early (dSph) and late (dIrr) types were selected in the Local Group, and are plotted in the colour–luminosity diagram together with the members of the NGC 524 group. The dwarfs of the Local Group and NGC 524 group occupy approximately the same colour interval; the reddest dwarf of the Local Group, Ursa Minor, is a dSph dwarf with $B - V = 1.3 \pm 0.3$, like the reddest dwarfs of the NGC 524 group. However, the bluest dwarfs of the Local Group are more luminous than the bluest dwarfs found near the large galaxies of the NGC 524 group, on average by approximately 2^m .

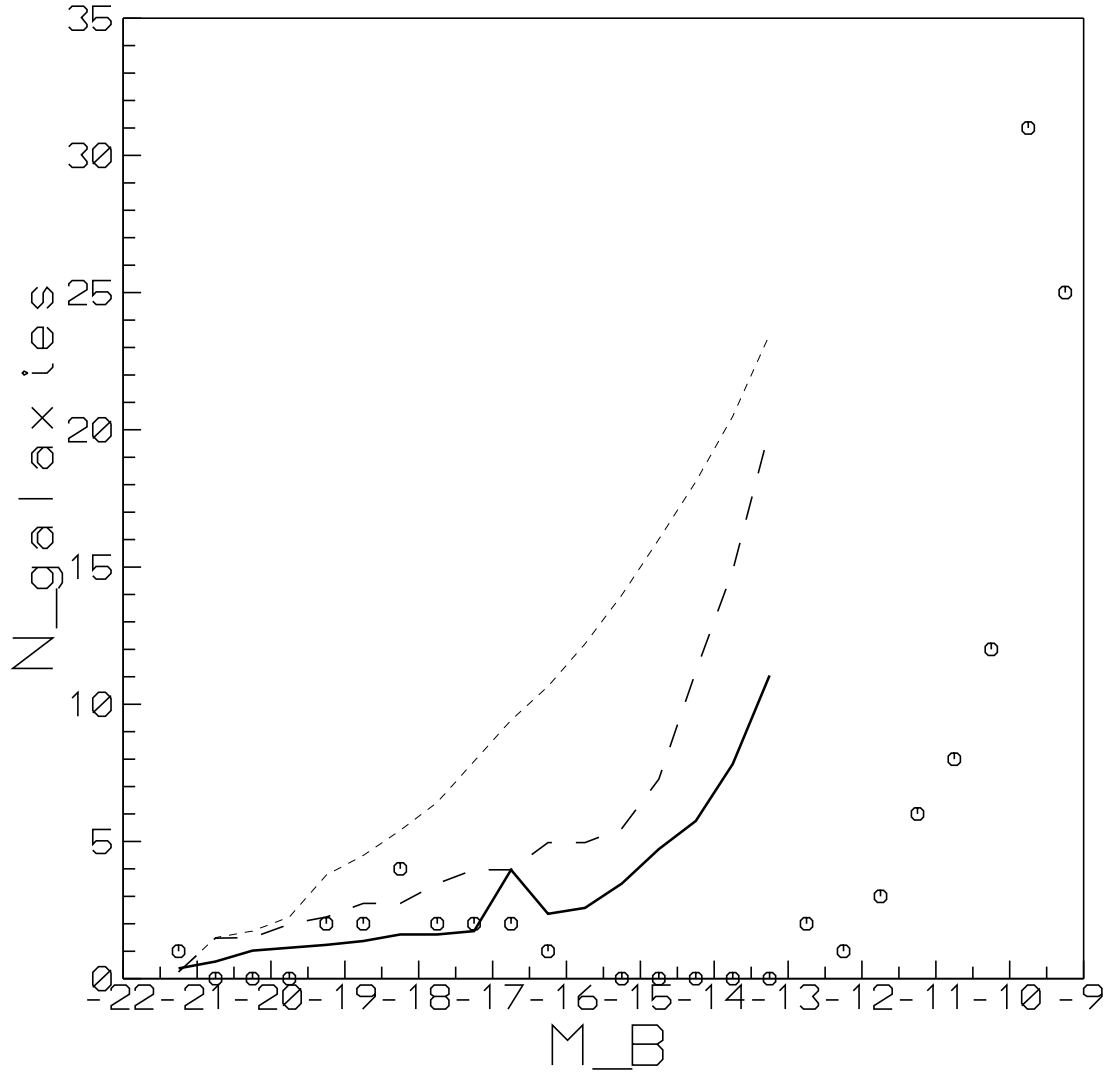


Figure 4: Luminosity function of the galaxies of the NGC 524 group in the range of $M_B = -22$ to -16 , following the data of [3], and in the range of $M_B = -13$ to -9 , following our measurements. For comparison, lines show the average luminosity functions of groups of different masses, according to [21]: massive groups with high X-ray luminosities (dotted line), groups with intermediate masses and low X-ray luminosities (dashed line), and groups without X-ray emitting gas (solid line).

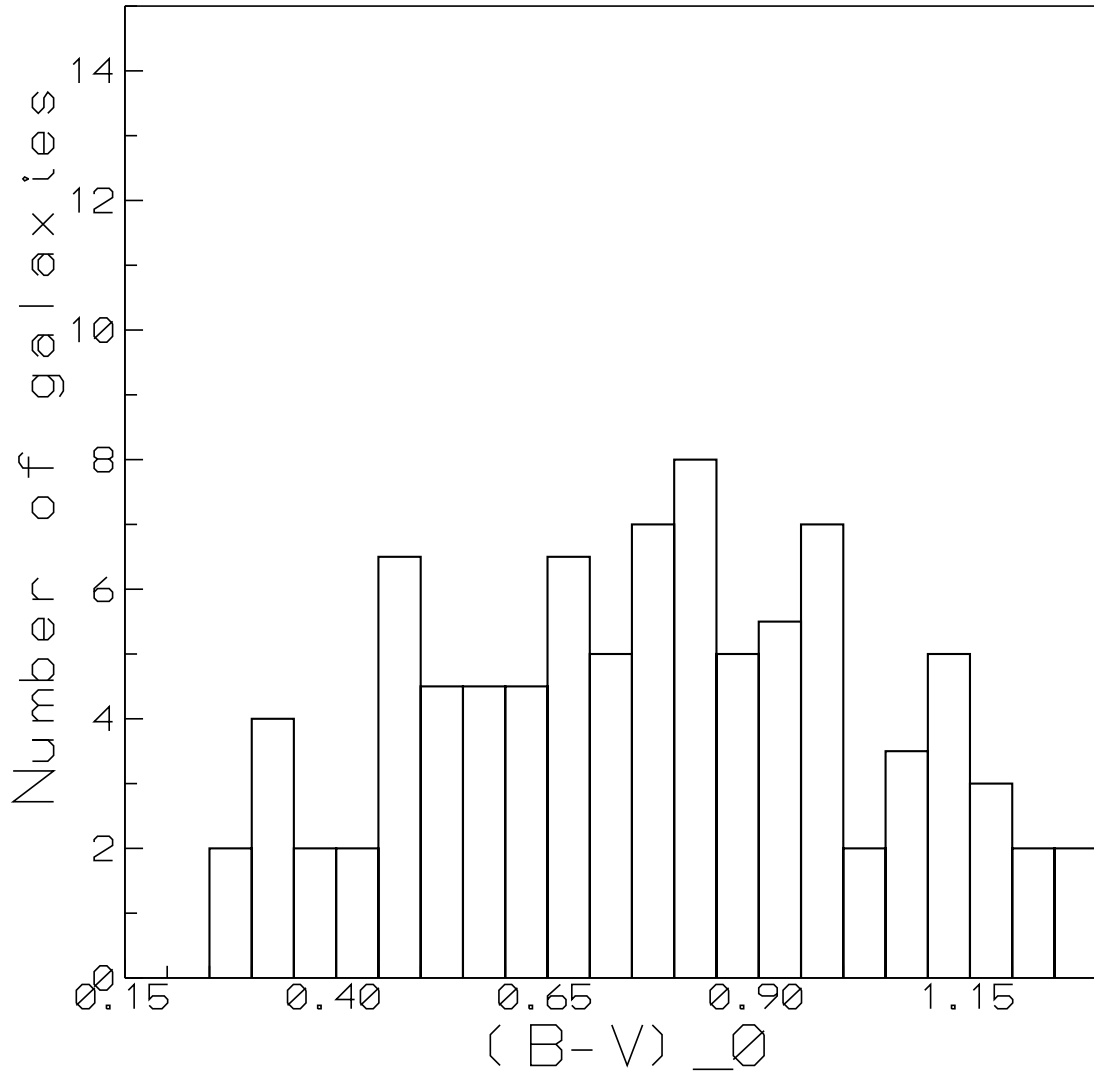


Figure 5: Distribution of dwarf galaxies of the NGC 524 group over their $B - V$ colours (corrected for the reddening in our Galaxy).

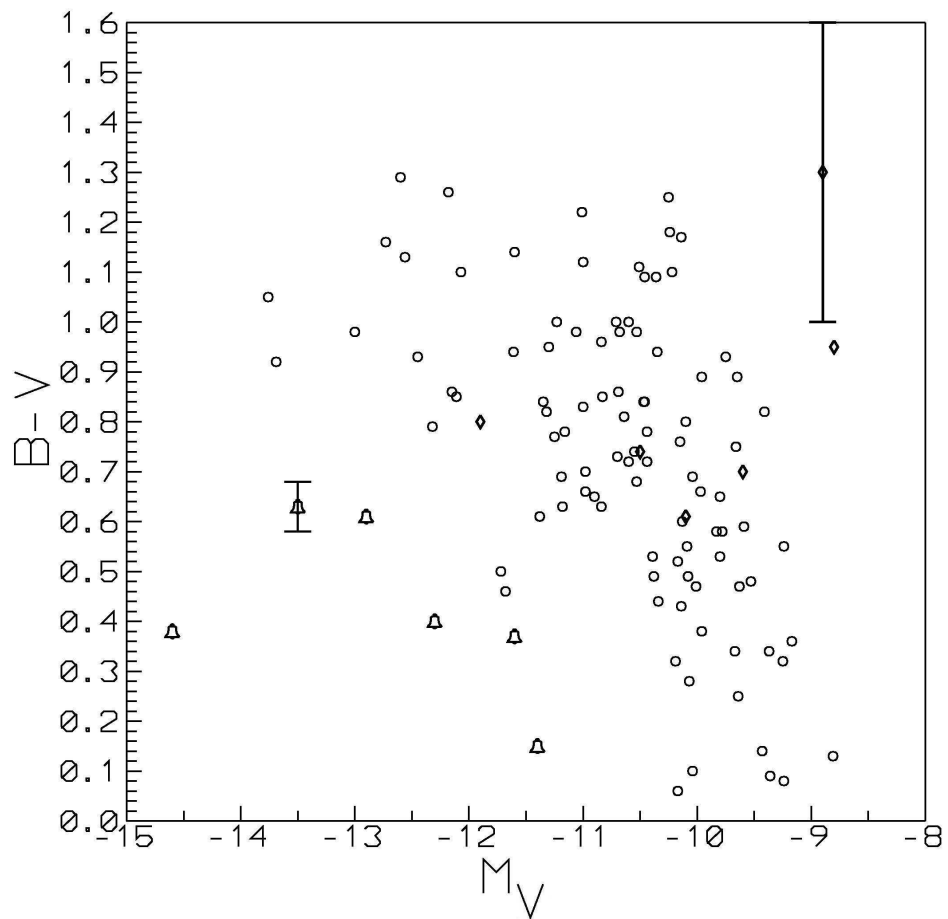


Figure 6: Colour-luminosity diagram for the dwarf galaxies of the NGC 524 group compared to dwarf galaxies of the Local Group. The circles show dwarf galaxies of the NGC 524 group, the bells – late-type dwarfs of the Local Group with young stellar populations, and the diamonds – dSph dwarfs of the Local Group with old stellar populations

5 CONCLUSIONS

We have analyzed the structures of the six largest disk galaxies of the NGC 524 group using surface photometry data obtained at the SAO 6-m telescope with the SCORPIO reducer. Four of the galaxies are classified in the literature as lenticular galaxies, and another two are classified as early-type spiral galaxies; two galaxies are viewed almost face-on, while the remaining four are inclined at large angles to the line of sight. As far as we can judge from their images, none of the galaxies viewed not quite edge-on has a large-scale bar. According to the behaviour of the radial surface-brightness distributions, the only galaxy that may contain a bar is NGC 516, which is viewed strictly edge-on; but, more probably, it is not a bar but an embedded, thin inner edge-on disk. In general, bars are present in 40%-70% of disk galaxies; their absence in all the large galaxies of the NGC 524 group could indicate some influence from their environment. However, we detected both inner and relative large outer rings in almost all the large disk galaxies in the NGC 524 group. In the face-on galaxies NGC 502 and NGC 524, rings of different radii fill out almost the entire range of radial distances. The nearby statistics of the frequency of bars in disk galaxies indicates that about 50% of such galaxies have inner rings [23], while 20% have nuclear rings (with radii out to 1.5 kpc) [24], with a bar being present in the overwhelming majority of galaxies with rings. The disk galaxies of the NGC 524 group have rings but no bars. It is interesting that no neutral hydrogen was found in the four lenticular galaxies of the group [9]; i.e., there is no gas and so no star formation, but there are rings (waves) of surface brightness. If such structural anomalies are to be explained by an enhanced contribution of secular evolution during the

formation of the large-scale structure of the galaxies in a dense environment, we must search for special mechanisms of the secular evolution that would not switch on star formation (for which there is no fuel in this case). Here we must also explain why the Sersic exponents of the bulges of all the group members are lower than two: bulges built via the secular evolution of disks with bars and gas may have exponential bulges, while “minor merging” (the capture of satellites) usually increases the Sersic exponents in bulges to 3–4 [25]. The presence of a large number of the blue dwarf galaxies undergoing current star formation within some 20–30 kiloparsec from the large galaxies of the group is interesting. Dynamical evolution over scales of a few billion years should cause these dwarfs to “fall” into their parent galaxies, or at least deprive them of gas and ongoing star formation, as in the Local Group. Thus, the systems of blue dwarfs around large red galaxies should either be systems recently assembled, or should be in stable orbits that prevent their falling into the centers of parent galaxies; otherwise, the continuous accretion of gas-rich dwarfs onto the disks of lenticular galaxies would provide the large galaxies with a fuel for ongoing star formation. Our spectral studies have shown that the outer disks of NGC 502 and NGC 524 have very old stellar populations [26], so this accretion does not occur for some reason.

The data used in this study were obtained at the 6-m telescope of the Special Astrophysical Observatory of the Russian Academy of Sciences, operated with financial support from the Ministry of Education and Science of the Russian Federation (registration number 01-43). We thank A.V. Moiseev for supporting these observations. The data analysis made use of the Lyon-Meudon Extragalactic Database (LEDA), maintained by the LEDA team at the Lyon Centre for Astrophysics Research (CRAL; France), and the

NASA/IPAC Extragalactic Database (NED), operated by the Jet Propulsion Laboratory of the California Institute of Technology under contract with the National Aeronautics and Space Administration (USA). We also used public data of the SDSS-III project (<http://www.sdss3.org>), supported by the Alfred P. Sloan Foundation, the participating institutions of the SDSS Collaboration, the National Science Foundation, and the U.S. Department of Energy Office of Science. This study was supported by the Russian Foundation for Basic Research (project no. 10-02-00062a).

References

- [1] J. Kormendy, R.C. Kennicutt Jr., *Ann. Rev. Astron. Astrophys.* **42**, 603 (2004)
- [2] M.J.Geller, J.P.Huchra, *Astrophys. J. Suppl. Ser.* **52**, 61 (1983)
- [3] J. Vennik, *Balt. Astronomy* **1**, 415 (1992)
- [4] S. Brough, D.A. Forbes, V.A. Kilborn, W. Couch, *MNRAS* **370**, 1223 (2006)
- [5] D. Makarov, I. Karachentsev, *MNRAS* **412**, 2498 (2011)
- [6] D.A. Forbes, T. Ponman, F. Pearce, et al., *Publ. of the Astron. Soc. of Australia* **23**, 38 (2006)
- [7] J. Osmond, T. Ponman, *MNRAS* **350**, 1511 (2004)
- [8] de Vaucouleurs G., de Vaucouleurs A. Corwin H.G., Jr., et al. "Third Reference Catalogue of Bright Galaxies. Volume I: Explanations and References". New York: Springer (1991)
- [9] Ch. Sengupta, R. Balasubramanyam, *MNRAS* **369**, 360 (2006)
- [10] J.L. Tonry, A. Dressler, J.P. Blakeslee, et al., *Astrophys. J.* **546**, 681 (2001)
- [11] V.L. Afanasiev, A.V. Moiseev, *Astron. Letters* **31**, 194 (2005)
- [12] K.C. Freeman, *Astrophys. J.* **160**, 767 (1970)
- [13] A.V. Moiseev , J.R. Valdés, V.H. Chavushyan, *A & A* **421**, 433 (2004)

- [14] P. Erwin, M. Pohlen, J.E. Beckman, *Astron. J.* **135**, 20 (2008)
- [15] L. Gutiérrez, P. Erwin, R. Aladro, J.E. Beckman, *Astron. J.* **142**, 145 (2011)
- [16] E. Laurikainen, H. Salo, R. Buta, J.H. Knapen, *Astrophys. J.* **692**, L34 (2009)
- [17] I. Katkov, I. Chilingarian, O. Sil'chenko, A. Zasov, V. Afanasiev, *Balt. Astronomy* **20**, 453 (2011)
- [18] D.J. Schlegel, D.P. Finkbeiner, M. Davis, *Astrophys. J.* **500**, 525 (1998)
- [19] D. Sowards-Emmerd, J.A. Smith, T.A. McKay, et al., *Astron. J.* **119**, 2598 (2000)
- [20] T.S. Chonis, C.M. Gaskell, *Astron. J.* **135**, 264 (2008)
- [21] T.A. Miles, S. Raychaudhury, D.A. Forbes, et al., *MNRAS* **355**, 785 (2004)
- [22] M.L. Mateo, *Ann. Rev. Astron. Astrophys.* **36**, 435 (1998)
- [23] R. Buta, F. Combes, *Fundamentals of Cosmic Physics* **17**, 95 (1996)
- [24] S. Comerón, J.H. Knapen, J.E. Beckman, et al., *MNRAS* **402**, 2462 (2010)
- [25] J.A.L. Aguerri, M. Balcells, R.F. Peletier, *A& A* **367**, 428 (2001)
- [26] O.K. Sil'chenko, I.S. Proshina, A.P. Shulga, S.E.Koposov, *MNRAS*, submitted